AGU PUBLICATIONS

Geophysical Research Letters

RESEARCH LETTER
10.1002/2016GL070014

Key Points:
- Martian large ripples dynamics are more similar to longitudinal dunes than impact ripples
- First evidence for longitudinal large ripple migration on Mars
- Martian large ripples consistently migrate in Gale Crater

Supporting Information:
- Supporting Information S1
- Movie S1
- Movie S2
- Movie S3
- Movie S4
- Movie S5

Correspondence to:
S. Silvestro,
silvestro@na.astro.it

Citation:
Silvestro, S., D. A. Vaz, H. Yizhaq, and F. Esposito (2016), Dune-like dynamic of Martian Aeolian large ripples, *Geophys. Res. Lett.*, *43*, 8384–8389, doi:10.1002/2016GL070014.

Received 13 JUN 2016
Accepted 5 AUG 2016
Accepted article online 9 AUG 2016
Published online 30 AUG 2016

Dune-like dynamic of Martian Aeolian large ripples

S. Silvestro[1,2], D. A. Vaz[3,4], H. Yizhaq[5], and F. Esposito[1]

[1]INAF Osservatorio Astronomico di Capodimonte, Naples, Italy, [2]SETI Institute, Carl Sagan Center, Mountain View, California, USA, [3]CITEUC Centre for Earth and Space Research of the University of Coimbra, Observatório Geofísico e Astronómico da UC, Santa Clara, Portugal, [4]CERENA Center for Natural Resources and the Environment, Instituto Superior Técnico, Lisbon, Portugal, [5]Department of Solar Energy and Environmental Physics, Ben-Gurion University of the Negev, Israel

Abstract Martian dunes are sculpted by meter-scale bed forms, which have been interpreted as wind ripples based on orbital data. Because aeolian ripples tend to orient and migrate transversely to the last sand-moving wind, they have been widely used as wind vanes on Earth and Mars. In this report we show that Martian large ripples are dynamically different from Earth's ripples. By remotely monitoring their evolution within the Mars Science Laboratory landing site, we show that these bed forms evolve longitudinally with minimal lateral migration in a time-span of ~six terrestrial years. Our observations suggest that the large Martian ripples can record more than one wind direction and that in certain cases they are more similar to linear dunes from a dynamic point of view. Consequently, the assumption of the transverse nature of the large Martian ripples must be used with caution when using these features to derive wind directions.

1. Study Area and Methods

In this study, we investigate the meter-scale aeolian bed forms sculpting the slopes of the informally named Bagnold dunes within the NASA Mars Science Laboratory landing site (Figure 1a) in Gale Crater. We will refer to these features as large ripples (LRs) or we will use the more generic term of "bed forms" because we will argue they may have a different dynamic to most known terrestrial aeolian ripples. The Bagnold dunes are elongated barchans and longitudinal dunes, morphologies consistent with a bidirectional wind regime [*Hobbs et al*., 2010; *Silvestro et al*., 2013]. These dunes are covered by three overlapping High-Resolution Imaging Science Experiment (HiRISE) images that are suitable for aeolian change detection studies (Figure S1 and Table S1 in the supporting information). We quantified the LR's migration rate in the *T*1–*T*3 time span ($\Delta T = 2075$ Earth days) using the "Co-registration of Optically Sensed Images and Correlation" (COSI-Corr) tool suite [*Leprince et al*., 2007]. The normalized misregistration error, which resulted from the coregistration and orthorectification process, was 0.03 ± 0.95 and 0.05 ± 1.39 pixels for the *T*1–*T*2 and *T*2–*T*3 pairs, respectively (more detail is provided in the supporting information). The COSI-Corr displacement maps are further improved by removing jitter artifacts (Figure S2). We then used the Object-based Ripple Analysis technique [*Vaz and Silvestro*, 2014] to characterize the directional distribution of the LRs, evaluate their spatial distribution and correlate bed form pattern characteristics with migration rates and morphometric settings [*Vaz and Silvestro*, 2014; *Vaz et al*., 2015] (Figure S3).

2. Results

Martian large ripples (wavelength, $\lambda = 1.9 \pm 0.2$ m) in the study area show a pervasive migration toward the SW and values of displacement reaching 1.7 m per Earth year (m/EY) (Figures 1a and 1b). Overall, the trend of the crestlines also reflects a bidirectional wind regime. Two sets of crestlines with modes at 41 and 322° intersect forming a mixed square pattern with transverse and longitudinal elements to the COSI-Corr vectors where individual crest terminations (junctions) are not recognizable (Figures 1c and 1d). Such a crestline arrangement is pervasive (~90% of the mapped area), but locally, the 41° bed forms are predominant and form a more regular pattern with evident Y junctions (Figure 1e). We investigate further the LR's pattern variability by looking at the degree of straightness of bed forms using the horizontal form index (*H* index), the ratio between the length and wavelength of the large bed forms [*Allen*, 1968]. In this paper, we use a modified version of the *H* index, the MH_{ind} (see supporting information) in order to segment the bed forms into two classes and evaluate their spatial distribution (Figures 2 and S3). We define a 3-D class ($MH_{ind} \leq 2$) and a 2-D class ($MH_{ind} > 2$), corresponding to the patterns that are more three-dimensional (shorter and irregular patterns, e.g., Figure 1c) or two-dimensional (bed forms presenting long and regular crests, e.g., Figure 1e)

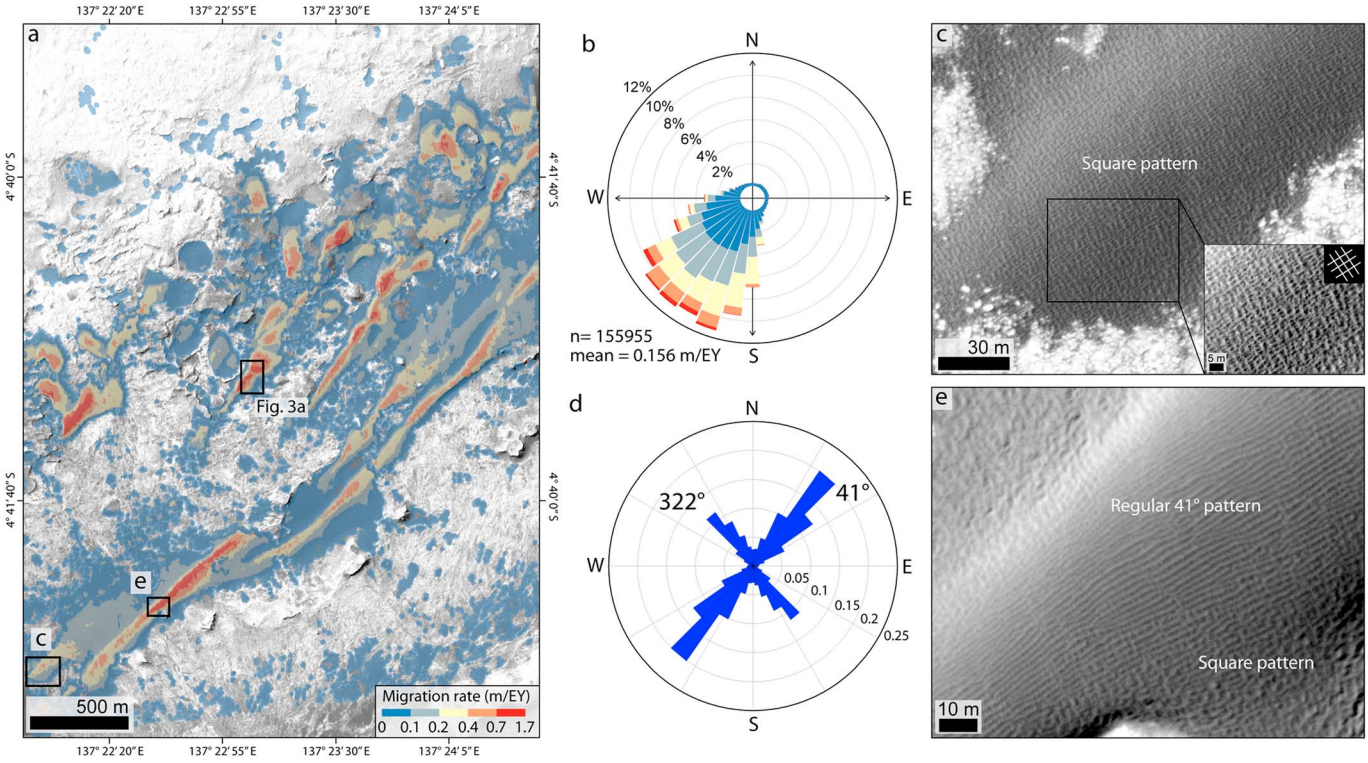

Figure 1. (a) COSI-Corr large ripple displacement map for the *T*1–*T*3 time range. In this map, individual displacement values are converted into migration rates (meter per Earth Year). (b) Circular distribution for all the COSI-Corr migration vectors (color coded by magnitude). (c) Large ripple mixed square pattern; both ripple crestlines are severely reworked with no Y junctions visible. (d) Large ripple length-weighted circular distribution denoting bimodality with two modes at 41° and 322°. (e) Large ripple morphological variability in the study area; the 41° bed forms are locally predominant and form a more regular pattern where individual junctions can be recognized.

(Figures 2a–2c and S4). Because LR's topography cannot be resolved by the DTM (Digital Terrain Model), inferences on the dimensionality of the ripples are based on terrestrial observations showing that 2-D bed forms have a constant height along the crestline, while complex and irregular ripple patterns do not [*Allen*, 1968, 1982; *Rubin*, 2012]. This analysis shows that the 2-D-class LRs are found in the following specific topographic settings: (1) on longitudinal dune elements (Figure 2a), (2) at higher dune elevations where the sediment transport rate is higher (Figures 2b–2f), and (3) on gently sloping surfaces (Figure S5).

Conversely, the 3-D bed form class dominates on lower dune elevations where the wind flow is more complex and where sand grains are not as well sorted as at the dune top (Figure 2) [*Pye and Tsoar*, 2009].

A closer inspection of the 2-D pattern reveals that these features are not stationary. The Y junctions (the termination of one bed form against another) moved toward the SW while the bed form crestlines displayed only limited lateral migration (Figure S6 and Movies S1–S5). Due to this particular and unique behavior, we focus on the 41° LR pattern dynamic. We manually mapped the movement of 52 junctions throughout the study area (Figure S6), and we digitized the corresponding bed form crestlines (Figures 3a and 3b). We only selected junctions that are unmistakably visible in all the three HiRISE frames (Movies S1–S5). In Figure 3c the displacement of 52 Y junctions (black arrow) is plotted together with the average bed form trend (in red) derived from the manual mapping procedure. The plots show longitudinal Y junction migrations during the whole *T*1–*T*3 period (Table S2).

3. Discussion and Implications

Bed form pattern analysis and recent models demonstrate that bed form interactions are similar across scales and environments, meaning that the pattern evolution for dunes and ripples should be comparable [*Kocurek et al.*, 2010; *Rubin*, 2012]. In fact, dunes and ripples follow the same rule of alignment as they both

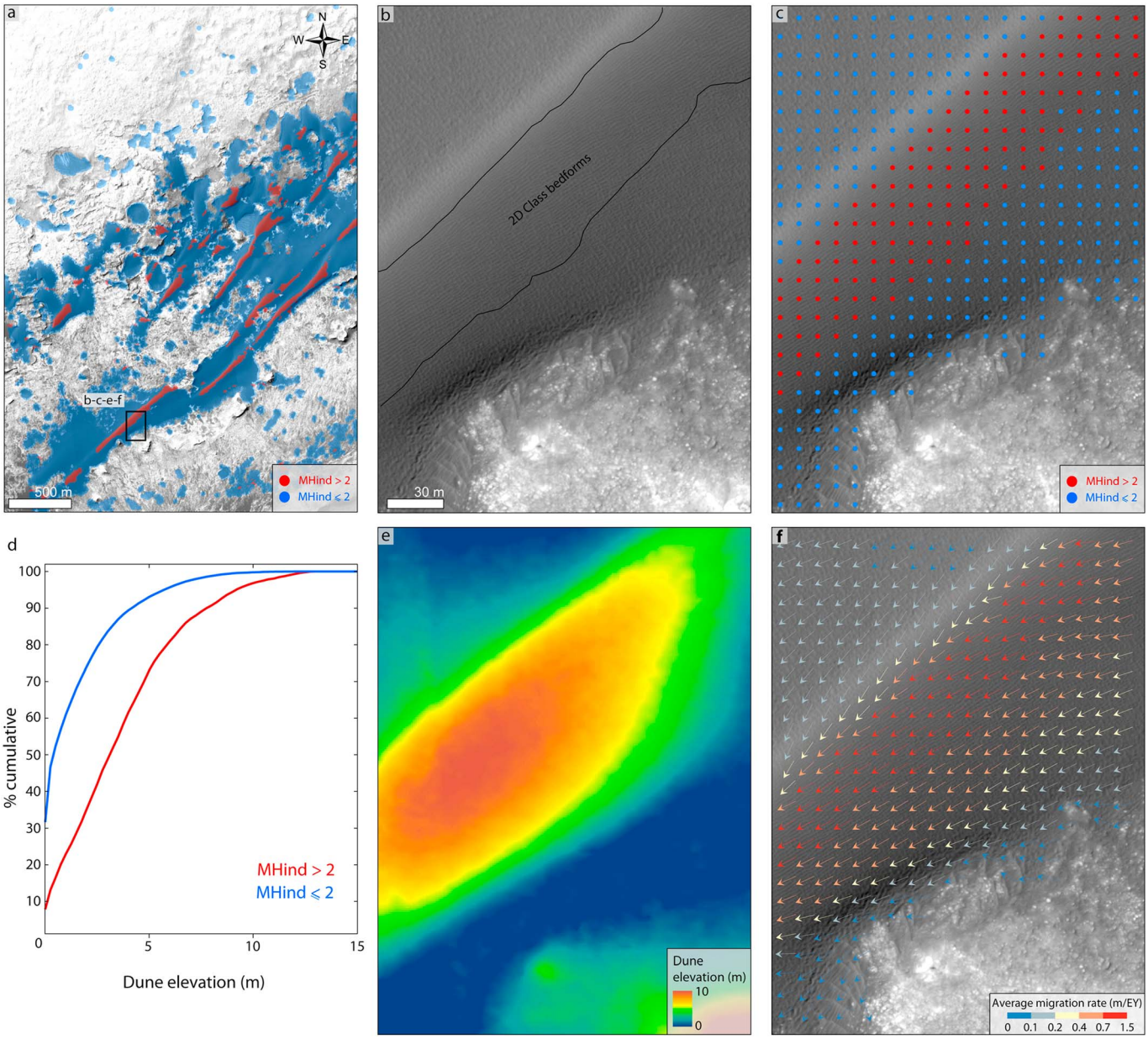

Figure 2. (a) The two large ripple populations distinguished visually can be segmented by using the modified *h* index. A three-dimensional bed form pattern (square pattern) in blue and a more regular two-dimensional bed form pattern in red. Note how the latter population is confined on longitudinal dune elements. (b) Zoom-in on the 2-D and 3-D bed form classes. (c) Mapped 2-D and 3-D bed form classes. (d) Cumulative frequencies for the two bed form classes plotted against dune elevation. Note how the 2-D-class large ripples ($MH_{ind} > 2$) are found at higher dune elevation. (e) HiRISE DTM highlighting the relationship between large ripple population and dune elevation. (f) COSI-Corr displacement vectors showing higher transport rates at higher dune elevations where the 2-D-class pattern occurs.

tend to maximize the gross bed form normal transport, in conditions in which the sediment supply is not a limiting factor [*Rubin and Ikeda*, 1990; *Courrech du Pont et al.*, 2014]. Thus, regardless of what type of bed form LRs are and what is the exact mechanism behind their formation [*Lapotre et al.*, 2016a, 2016b], we can speculate on the formative wind regime by just looking at the pattern's evolution. Direct observations and computer simulations of transverse bed forms in unidirectional flow show that the migration of Y junctions is always perpendicular to the bed form trend [*Werner and Kocurek*, 1999; *Yizhaq et al.*, 2004; *Reffet et al.*, 2010a; *Lorenz*, 2011]. Hence, the observed longitudinal Y junction displacements indicate along-crest sand movement which is typical of longitudinal bed forms [*Reffet et al.*, 2010a; 2010b, Movies SM2–SM4].

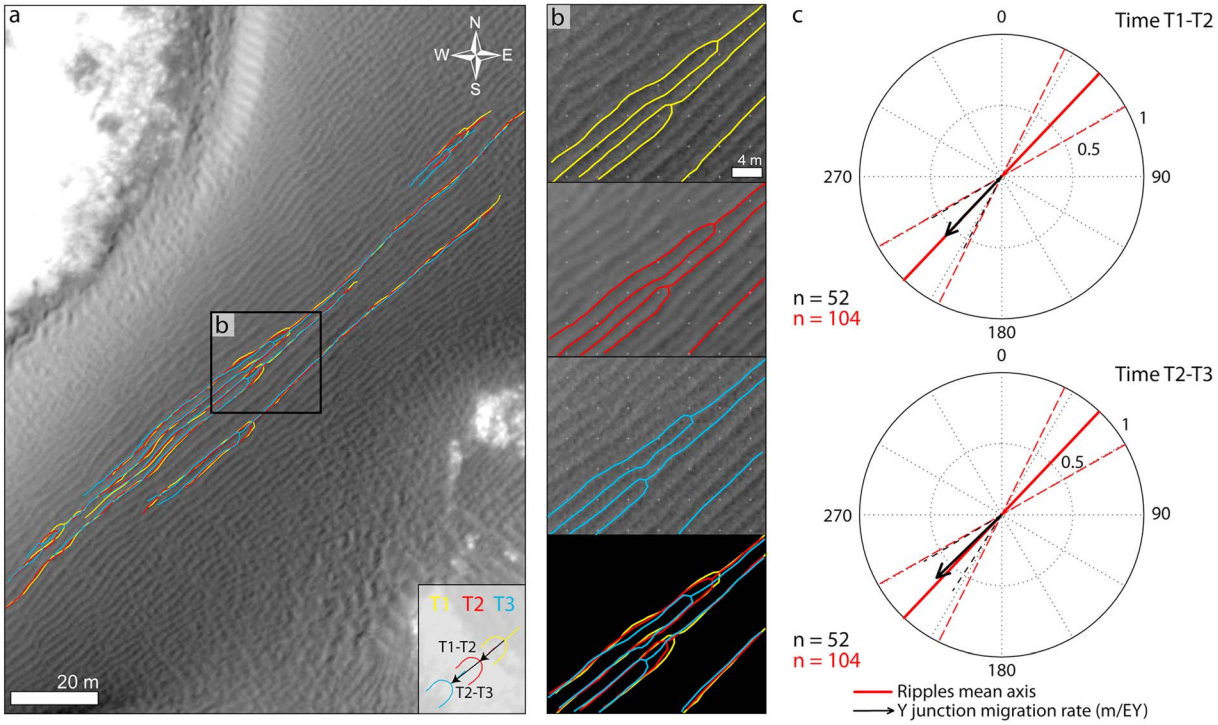

Figure 3. (a) Longitudinal migration of the LRs at *T*1–*T*3. (b) Zoom-in showing the longitudinal Y junction migration in the three frames. (c) Circular plot showing the comparison between the mean average Y junction migrations (in meter) and the mean bed form trend (circular standard deviation intervals are also shown) in the two study periods *T*1–*T*2 and *T*2–*T*3. Note that the Y junction migration direction is nearly longitudinal to the mean bed form trend and that the rate of migration is similar in the two analyzed intervals.

The effect of gravity acting on high sloping surfaces (>20° [*Liu and Zimbelman*, 2015]) can promote the formation of bed forms that are oblique or longitudinal to the formative wind direction [*Howard*, 1977]. However, this is unlikely to happen in our study area as most of the 2-D bed forms are located on gently sloping surfaces (Figure S5). Therefore, a bidirectional wind regime must be responsible for the formation of the longitudinal large ripples (however, we cannot rule out the effect of sediment cohesiveness which might also influence bed form alignment and evolution [*Rubin and Hesp*, 2009; *Yizhaq et al*., 2014]).

The square 3-D pattern could be the result of reworking (Figure 4a). In this scenario, a first wind from the NW or the SE formed the 41° bed forms. Then, during the *T*1–*T*3 period, the wind regime changed and winds from the NE formed the 322° pattern (Figure 4a). Alternatively, a bidirectional flow regime with a divergence angle close to 90° and with the two flows transporting the same amount of sediment (transport ratio equal to 1) may cause the observed 3-D bed form pattern [*Goossens*, 1991; *Reffet et al*., 2010a; *Rubin*, 2012] (Figure 4b). The proposed flow configurations can explain the 3-D LR pattern but is not valid for the 2-D-class bed forms; in particular, the Figure 4a scenario implies that areas subject to the most intense sand transport should show a higher degree of reworking (smoothed 41° crests and higher concentration of 322° bed forms), which is not what we see. Then, the alternative flow setting sketched in Figure 4b would create a pattern where transverse and longitudinal elements are present in equal proportion [*Rubin*, 2012]. Therefore, the wind regime atop of the dunes should be different. Here we postulate that a bidirectional flow regime with a divergence angle higher than 90° [*Reffet et al*., 2010a; *Rubin*, 2012] is responsible for the 2-D pattern formation (Figure 4c). In this scenario, the higher divergence angle favors the predominance of the 41° longitudinal bed forms, which aligns with the resultant transport directions (Figure 4c). Consequently, the pattern is less reworked and more two-dimensional. Because the orientation of the 2-D large ripples matches the trend of the longitudinal dunes they superimpose, the winds shaping the large ripples are likely the same that shape the dunes in the long term. Strikingly, the reported Y junction's dynamic is the same observed for longitudinal dunes obtained in the water tank [see also *Reffet et al*., 2010b, Movies SM4 and SM6].

Longitudinal dunes are the most widespread morphologies on Earth [*McKee*, 1979; *Pye and Tsoar*, 2009]. Conversely, as far as we know, longitudinal wind ripples have never been reported from fieldwork.

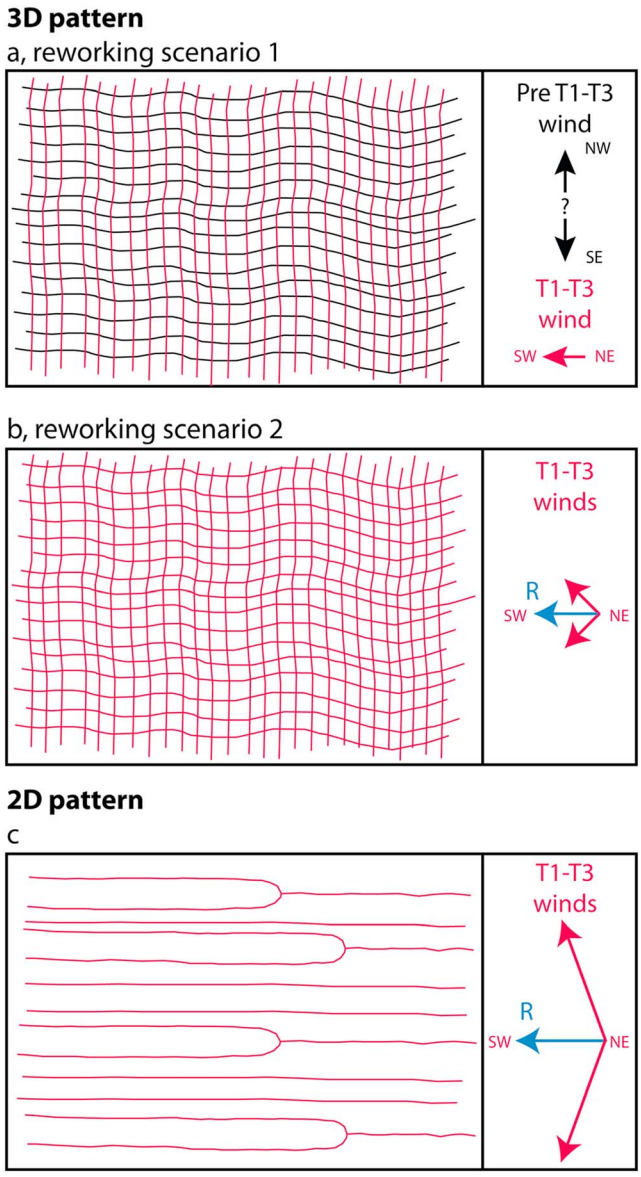

Figure 4. (a) Potential 3-D LRs pattern flow configuration. A first wind blowing from the NW or the SE formed the 41° LR set which was subsequently reworked by the 322° LRs during the *T*1–*T*3 period by a wind blowing from the NE. (b) Alternative 3-D pattern flow configuration where both LR sets are contemporaneous and were formed by two oblique winds with divergence angle equal to 90° and transport ratio equal to 1. (c) Possible flow configuration leading to the formation of the 2-D-class longitudinal ripples set with two winds blowing with high divergence angle (>90°) and with the junctions moving in the direction of the resultant transport direction (in blue).

Experimental studies show that longitudinal aeolian ripples can form in a bidirectional wind regime when each wind cycle is shorter than the ripple reconstitution time which is the time needed to adjust to new wind conditions [*Rubin and Hunter*, 1987; *Rubin and Ikeda*, 1990]. In other words, ripples should not be in phase with the last sand-blowing wind but rather in equilibrium with the time averaged properties of the airflow [*Rubin and Ikeda*, 1990]. On Earth, sand dunes in air and water usually fit this scenario while normal aeolian impact ripples often do not [*Goossens*, 1991], as these small bed forms ($\lambda < 30$ cm) can be quickly oriented with the last wind direction. On the other hand, the Martian environment, with few winds capable to move sand [*Moore*, 1985; *Kok*, 2010] and large meter-scale bed forms with high reconstitution time, promotes the existence of oblique and longitudinal features. Therefore, because the Martian large ripples can integrate the effects of more than one wind direction, they are similar to dunes from a dynamic point of view, and this has several implications. First of all, care should be taken when reconstructing the wind regime from the orientations of the Martian large ripples [*Silvestro et al.*, 2011; *Liu and Zimbelman*, 2015] and when using these features to back-model winds over the dunes, especially in areas where the wind regime is not strictly unidirectional [*Jackson et al.*, 2015]. In addition, because oblique and longitudinal LRs should be common on Mars, deriving paleowind directions from ancient sandstones might not be straightforward [*Rubin and Hunter*, 1981, 1985]. Preliminary results from the Curiosity rover data suggest that the sinuous large ripples visited at the base of the Namib dune might be fluid-drag ripples [*Lapotre et al.*, 2016a, 2016b]. Our results based on multitemporal HiRISE image analysis indicate that other explanations than the impact/splashing mechanism need to be found to clarify the Martian large ripple presence. In particular, the hypothesis that the instability leading to the formation of these features is aerodynamic in nature cannot be ruled out.

Finally, we show that sand movement in Gale is not limited to the SW dune field sector [*Silvestro et al.*, 2013] and that more modeling efforts are needed to correctly predict and reproduce sand saltation events on Mars

[*Rafkin et al*., 2016]. By combining camera images with the Rover Environmental Monitoring Station measurements, Curiosity will have a unique opportunity to validate our hypothesis and track the first evidence for longitudinal large ripple migration ever observed from the surface.

Acknowledgments
This work has been supported by ASI through the ASI-CISAS agreement I/018/12/0: "DREAMS EDM Payload - ExoMars 2016". The development of the DREAMS instrument was funded and coordinated by ASI under the leadership of INAF-Naples, Italy. S. Silvestro acknowledges Ian Walker (ASU) and Serina Diniega (JPL) for providing useful advice, comments, and for English editing. D.A. Vaz was supported by FCT with the grant FRH/BPD/72371/2010 and the contracts UID/Multi/00611/2013 and COMPETE2020/POCI-01-0145-FEDER-006922. We all acknowledge N.T. Bridges, M. Chojnacki, A. Fennema, and S. Sutton for providing the balanced cubes used as input for the COSI-Corr processing. J. Zimbelman and J. Randebaugh are also acknowledged for their constructive review. The data used in this paper can be accessed upon personal request to the first author (silvestro@na.astro.it).

References

Allen, J. R. L. (1968), *Current Ripples: Their Relation to Patterns of Water and Sediment Motion*, North-Holland, Amsterdam.
Allen, J. R. L. (1982), *Sedimentary Structures, their Character and Physical Basis*, vol. 1, edited by J. R. L. Allen, Elsevier Sci, Amsterdam.
Courrech du Pont, S., C. Narteau, and X. Gao (2014), Two modes for dune orientation, *Geology*, *44*, 743–746, doi:10.1130/G35657.1.
Goossens, D. (1991), Superposition of aeolian dust ripple patterns as a result of changing wind directions, *Earth Surf. Processes Landforms*, *16*, 689–699.
Hobbs, S. W., D. J. Paull, and M. C. Bourke (2010), Aeolian processes and dune morphology in Gale Crater, *Icarus*, *210*(1), 102–115, doi:10.1016/j.icarus.2010.06.006.
Howard, A. D. (1977), Effect of slope on the treshold of motion and its application to orientation of wind ripples, *Geol. Soc. Am. Bull.*, *88*, 853–856, doi:10.1130/0016-7606(1977)88<853.
Jackson, D. W. T., M. C. Bourke, and T. A. G. Smyth (2015), The dune effect on sand-transporting winds on Mars, *Nat. Commun.*, *6*, 8796, doi:10.1038/ncomms9796.
Kocurek, G., R. C. Ewing, and D. Mohrig (2010), State of Science How do bedform patterns arise? New views on the role of bedform interactions within a set of boundary conditions, *Earth Surf. Processes Landforms*, *63*, 51–63, doi:10.1002/esp.
Kok, J. F. (2010), An improved parameterization of wind-blown sand flux on Mars that includes the effect of hysteresis, *Geophys. Res. Lett.*, *37*, L12202, doi:10.1029/2010GL043646.
Lapotre, M. G. A., et al. (2016a), Large wind ripples on Mars: A record of atmospheric evolution, *Science*, *353*(6294), 55–58, doi:10.1126/science.aaf3206.
Lapotre, M., R. C. Ewing, M. Lamb, W. W. Fischer, K. W. Lewis, M. Ballard, M. D. Day, D. M. Rubin, and J. P. Grotzinger (2016b), Orbital and in-situ observations in support of the existence of an unknown stable aeolian bedform regime on Mars, in *47th Lunar and Planetary Science Conference*, LPI Contribution No. 1903, p. 1510, The Woodlands, Tex.
Leprince, S., S. Barbot, F. Ayoub, and J. P. Avouac (2007), Automatic, precise, ortho-rectification and coregistration for satellite image correlation, application to ground deformation measurement, *IEEE J. Geosci. Remote Sens.*, *45*(6), 1529–1558.
Liu, Z. Y. C., and J. R. Zimbelman (2015), Recent near-surface wind directions inferred from mapping sand ripples on Martian dunes, *Icarus*, *261*, 169–181, doi:10.1016/j.icarus.2015.08.022.
Lorenz, R. D. (2011), Observations of wind ripple migration on an Egyptian seif dune using an inexpensive digital timelapse camera, *Aeolian Res.*, *3*(2), 229–234, doi:10.1016/j.aeolia.2011.01.004.
McKee, E. D. (1979), *A Study of Global Sand Seas*, edited by E. D. McKee, *U.S. Geol. Surv. Prof. Pap.*, 1052.
Moore, H. J. (1985), The Martian dust storm of Sol 1742, *J. Geophys. Res.*, *90*, D163–D174, doi:10.1029/JB090iS01p00163.
Pye, K., and H. Tsoar (2009), *Aeolian Sand and Sand Dunes*, Springer, Berlin.
Rafkin, S. C. R., J. Pla-Garcia, M. Kahre, J. Gomez-Elvira, V. E. Hamilton, M. Mercedes, S. Navarro, J. Torres, and A. R. Vasavada (2016), The meteorology of Gale Crater as determined from Rover Environmental Monitoring Station observations and numerical modeling. Part II: Interpretation, *Icarus*, 1–25, doi:10.1016/j.icarus.2016.03.013.
Reffet, E., S. Courrech Du Pont, P. Hersen, and S. Douady (2010a), Formation and stability of transverse and longitudinal sand dunes, *Geology*, *38*(6), 491–494, doi:10.1130/G30894.1.
Reffet, E., S. Courrech Du Pont, P. Hersen, and S. Douady (2010b), Formation and stability of transverse and longitudinal sand dunes, GSA data repository 2010144, *Geology*, *38*(6), 491–494.
Rubin, D. M. (2012), A unifying model for planform straightness of ripples and dunes in air and water, *Earth Sci. Rev.*, *113*(3-4), 176–185, doi:10.1016/j.earscirev.2012.03.010.
Rubin, D. M., and H. Ikeda (1990), Flume experiments on the alignment of transverse, oblique, and longitudinal dunes in directionally varying flows, *Sedimentology*, *37*(4), 673–684.
Rubin, D. M., and P. A. Hesp (2009), Multiple origins of linear dunes on Earth and Titan, *Nat. Geosci.*, *2*, 653–658, doi:10.1038/NGEO610.
Rubin, D. M., and R. E. Hunter (1981), Reconstructing bedform assemblage from compound crossbedding, in *Eolian Sediments and Processes*, edited by M. E. Brookfield and T. S. Ahlbrandt, pp. 407–427, Elsevier, Amsterdam.
Rubin, D. M., and R. E. Hunter (1985), Why deposits of longitudinal dunes are rarely recognized in the geologic record, *Sediment. Geol.*, *32*, 147–157.
Rubin, D. M., and R. E. Hunter (1987), Bedform alignment in directionally varying flows, *Science*, *237*(4812), 276–278, doi:10.1126/science.237.4812.276.
Silvestro, S., D. A. Vaz, L. K. Fenton, and P. E. Geissler (2011), Active aeolian processes on Mars: A regional study in Arabia and Meridiani Terrae, *Geophys. Res. Lett.*, *38*, L20201, doi:10.1029/2011GL048955.
Silvestro, S., D. A. Vaz, R. C. Ewing, A. P. Rossi, L. K. Fenton, T. I. Michaels, J. Flahaut, and P. E. Geissler (2013), Pervasive aeolian activity along rover Curiosity's traverse in Gale Crater, Mars, *Geology*, *41*(4), 483–486, doi:10.1130/G34162.1.
Vaz, D. A., and S. Silvestro (2014), Mapping and characterization of small-scale aeolian structures on Mars: An example from the MSL landing site in Gale Crater, *Icarus*, *230*, 151–161, doi:10.1016/j.icarus.2013.08.007.
Vaz, D. A., P. T. K. Sarmento, M. T. Barata, L. K. Fenton, and T. I. Michaels (2015), Object-based dune analysis: Automated dune mapping and pattern characterization for Ganges Chasma and Gale crater, Mars, *Geomorphology*, *250*, 128–139, doi:10.1016/j.geomorph.2015.08.021.
Werner, B. T., and G. Kocurek (1999), Bedform spacing from defect dynamics, *Geology*, *27*, 727–730, doi:10.1130/0091-7613(1999)027<0727.
Yizhaq, H., N. J. Balmforth, and A. Provenzale (2004), Blown by wind: Nonlinear dynamics of aeolian sand ripples, *Phys. D Nonlinear Phenom.*, *195*(3-4), 207–228, doi:10.1016/j.physd.2004.03.015.
Yizhaq, H., J. F. Kok, and I. Katra (2014), Basaltic sand ripples at Eagle Crater as indirect evidence for the hysteresis effect in Martian saltation, *Icarus*, *230*, 143–150, doi:10.1016/j.icarus.2013.08.006.